

Calculation of the optical spectra of β' -NiAl and CoAl

Kwang Joo Kim, B. N. Harmon, and D. W. Lynch

Department of Physics and Ames Laboratory, U.S. Department of Energy, Iowa State University, Ames, Iowa 50011

(Received 29 August 1990)

Band structures of β' -NiAl and CoAl have been calculated to interpret the experimental optical spectra. The optical transitions of both compounds are calculated as direct interband transitions including electric-dipole matrix elements between the eigenstates of the ground state of the system. All of the structures found in the optical spectra of both compounds involve states with some Ni or Co d character in both the initial and the final states. The overall agreement is good between the calculated spectrum and the optical data for β' -NiAl. For β' -CoAl there is qualitative agreement but some discrepancy for the energy positions and the intensities of the structures. A self-energy correction for the excitation spectrum has been used for β' -CoAl to improve the agreement.

I. INTRODUCTION

The $3d$ transition metals Ni and Co form stable alloys with Al over a wide range of composition. These alloys form in the β' phase near stoichiometry in which they are ordered in the CsCl crystal structure. In the Al-poor region of the β' phase, Ni or Co atoms substitute on Al sites while in the Al-rich region vacancies are formed at Ni or Co sites. The electronic structures of β' -NiAl and CoAl have been studied extensively both theoretically and experimentally because of the simplicity of their crystal structure and the variation of physical properties that are made possible by the width of the β' -phase range.

Optical-spectroscopic measurements have provided information about the electronic structures of these alloys. Earlier, reflectivities of these alloys were measured and changes in the spectral features were found as the Al concentration varied.^{1,2} The dielectric functions of ordered β' -phase samples of both alloys were measured at room temperature by polarimetric techniques.^{3,4} Also, the optical absorptivity of β' -NiAl (Ref. 5) and CoAl (Ref. 6) were measured at 4.2 K using a calorimetric technique and dielectric functions were obtained by Kramers-Kronig (KK) analysis.

The electronic band structures of both compounds have been calculated a number of times⁷⁻¹¹ and the results were compared with the measured optical properties,^{7,10,11} soft-x-ray spectra,^{9,12} and photoemission spectra.¹³⁻¹⁵

In the present work, emphasis is placed on the calculation of the band structures and the resultant optical properties of β' -NiAl and CoAl under the assumption of direct (\mathbf{k} -conserved) interband transitions. We evaluate the real part of the optical conductivity as

$$\sigma_1 = \frac{\pi e^2}{3m^2\omega} \sum_{fi} \int_{\text{BZ}} d^3k \frac{2}{(2\pi)^3} |\mathbf{P}_{fi}|^2 \times \delta(E_f(\mathbf{k}) - E_i(\mathbf{k}) - \hbar\omega), \quad (1)$$

with

$$\mathbf{P}_{fi} = \frac{\hbar}{\Omega i} \langle f | \nabla | i \rangle, \quad (2)$$

where BZ denotes Brillouin zone and \mathbf{P}_{fi} is the electric-dipole matrix element between the occupied $E_i(\mathbf{k})$ and unoccupied $E_f(\mathbf{k})$ one-electron states calculated by using the corresponding ground-state one-electron wave functions. In Sec. II the calculated optical spectra are compared with experimental data and the transitions responsible for the structures in the spectra are identified.

II. CALCULATIONAL RESULTS AND DISCUSSION

β' -NiAl and CoAl have the CsCl structure in which the Bravais lattice is sc , the space group is O_h^1 , and the structure has two atoms per unit cell. The self-consistent band structures of both compounds were calculated using a scalar-relativistic version of the linearized-augmented-plane-wave (LAPW) method¹⁶ in which the Dirac equation is reduced to omit initially the spin-orbit interaction (thus keeping spin as a good quantum number but retaining all other relativistic kinematic effects). The spin-orbit interaction is added perturbatively after the semirelativistic bands and wave functions have been obtained. The muffin-tin approximation was used for the crystal potential and the exchange-correlation contribution to the potential was calculated by using the local-density approximation of Hedin and Lundqvist¹⁷ to the density-functional formalism. The muffin-tin sphere radii of Ni and Co were chosen so that the spheres surrounding their

TABLE I. Parameters used in the band calculations.

	NiAl	CoAl
Lattice constant (Å)	2.880	2.861
Muffin-tin radius (Å)	Ni 1.270 Al 1.193	Co 1.270 Al 1.193
Zero of potential (Ry)	-0.767	-0.784

sites extended 51% of the way to the Al sites. With this arrangement 66% and 67% of the unit-cell volumes are occupied by the muffin-tin spheres for NiAl and CoAl, respectively.

The size of the LAPW basis function set for each calculation was set to satisfy $K_{\max}R_{\text{MT}}=7.0$ for the smallest muffin-tin radius R_{MT} . This yielded about 60–80 LAPW's for both compounds depending on the k point. Inside R_{MT} , the wave functions were expanded in terms of spherical harmonics of angular momentum up to $l=12$. There were 56 k points in the $\frac{1}{48}$ th of the BZ, included for the self-consistent iterations. The parameters used for this work are listed in Table I.

Figures 1 and 2 show the band structures of β' -NiAl and CoAl, respectively, calculated relativistically including the spin-orbit interaction along some high-symmetry directions. For both compounds, inclusion of the relativistic effects do not shift or split the energy spectra significantly on the scale of the figures, so that our results are not so different from other authors' results,^{7–11} which did not consider relativistic effects. It is seen that both band structures look very similar except for the energy positions of the relatively flat bands near the Fermi level E_F . As shown in Fig. 3 the densities of states of level both compounds also look similar to each other except for the relative position of E_F to the high-density peaks which are due to the flat bands. These peaks are caused by narrow d bands of Ni or Co. It is also seen that with one additional electron per cell the Fermi level of NiAl is located about 0.5 eV above that of CoAl relative to the structure in the bands. The smaller peaks near E_F (below E_F for NiAl and above E_F for CoAl) are composed of states with predominantly d character. The d bands are essentially filled in NiAl while there is still some density of d states above E_F in CoAl.

Calculations of the optical conductivities σ_1 of both compounds were performed using the linear-energy-

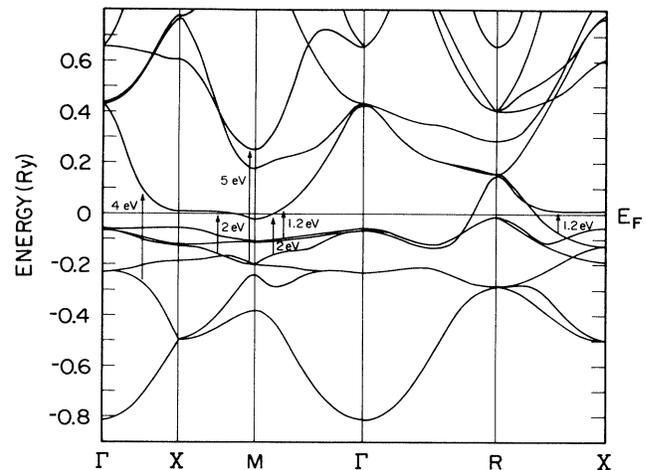


FIG. 2. Relativistic energy band structure of β' -CoAl.

tetrahedron method.¹⁸ In calculating σ_1 as in Eq. (1), the energy eigenvalues were evaluated at the four corners of 286 elementary tetrahedra in the irreducible $\frac{1}{48}$ th of the sc BZ, and the electric-dipole matrix elements were calculated as in Eq. (2) using the wave functions at the centers of the tetrahedra. We assumed the electric-dipole matrix elements to be constant within a tetrahedron and equal to the matrix element calculated at the center. The calculated spectra were then convoluted with an energy-dependent Lorentzian broadening function of width described by $\Gamma(E)=0.05E^2$, with E the energy in eV, to account for the experimental resolution.

In Fig. 4 the calculated σ_1 of β' -NiAl is shown and compared with the optical data obtained from KK analysis of the absorptivity, $A=1-R$, with R the reflectivity, measured at 4.2 K in the energy range of 0.2–4.4 eV using a calorimetric technique⁵ which is ad-

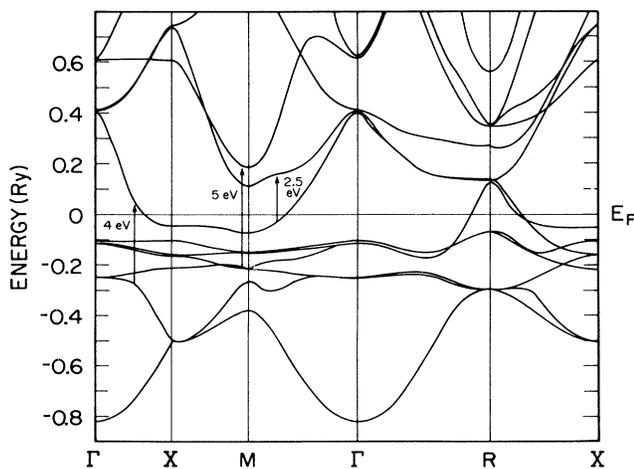


FIG. 1. Relativistic energy band structure of β' -NiAl.

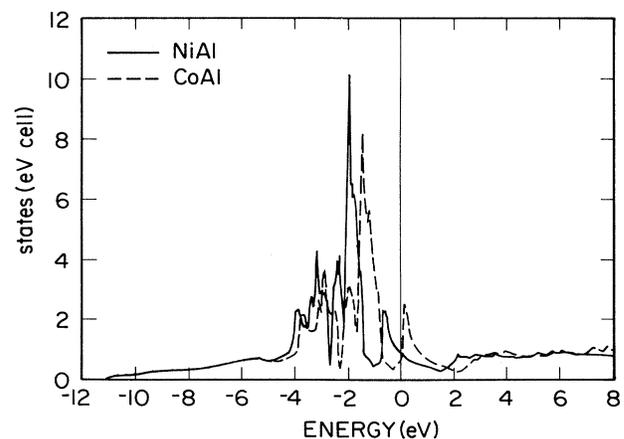


FIG. 3. Densities of states of β' -NiAl and CoAl.

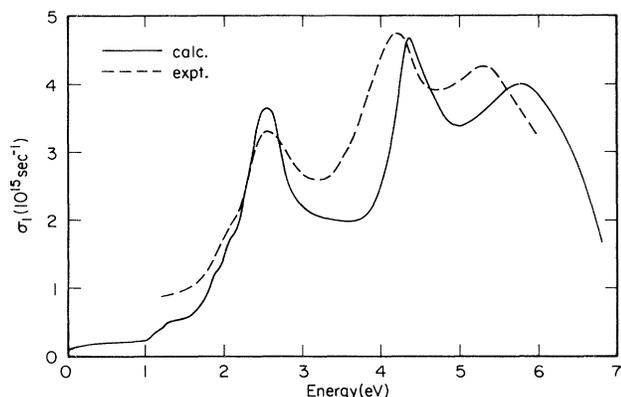


FIG. 4. Comparison of the calculated optical conductivity with the experimental data for β' -NiAl.

vantageous for resolving small structures at lower energies due to interband transitions by reducing the background in the dielectric function caused by phonon-assisted intraband transitions that grow as the temperature rises. The intraband (Drude) contribution to the optical data which provides a decreasing and structureless background as the energy increases is not subtracted. Plotting σ_1 instead of the dielectric function (ϵ_2) emphasizes the interband term with respect to the Drude term. In the KK analysis of the measured reflectivity, a Drude term below 0.2 eV, room-temperature reflectivity data of Ref. 2 between 4.4 and 5.6 eV, a shifted average of Ni (Ref. 19) and Al (Ref. 20) reflectivity data between 5.6 and 27 eV, and a power-law function above 27 eV were used.

The calculational results show that interband transitions start as low as 0.2 eV between states with mostly Ni p - d character around the R point, where two bands are located close to each other across E_F , as can be seen along the R - X direction in Fig. 1. At higher energies there are two prominent peaks at about 2.5 and 4.3 eV with a shoulder at about 2.0 eV. It is seen that the positions and intensities of these calculated structures agree well with the measured optical spectrum, which shows structures at about 2.0, 2.5, and 4.2 eV. At low energies (< 1.5 eV) the measured optical data increase rapidly so that the interband transitions, although they contribute, may not be resolved from the background of intraband transitions, as is evident in the optical data^{3,5} measured at room temperatures. The contributions to the 2.0-eV structure come from transitions involving states with Ni p - d character near E_F as initial or final states. The major contribution to the 2.5-eV structure comes from transitions between initial states with Ni p - d and Al p character near E_F and final states above E_F with Ni s - p - d and Al s character (e.g., bands 7 and 8 in the Γ - M direction, respectively). The 4-eV structure is mostly due to transitions between states with Ni p - d character mixed with Al p character well below E_F and near E_F (e.g., bands 2 and

7 in the Γ - X direction, respectively).

The regions in the BZ that have major contributions to the structures in σ_1 were found by calculating Eq. (1) for each of the 220 tetrahedra for selected energy windows centered at the peaks of each structure. The intensities of all the interband transitions having energy differences between initial and final states falling in the energy window were summed for each tetrahedron to represent the contribution from the tetrahedron to the structure. Figure 5 shows the distributions of the transition intensities for the 2.5- and 4-eV structures of NiAl in the $\frac{1}{48}$ th of the BZ. Each tetrahedron is represented by a parallelogram if it makes a contribution to the structure, with the size of the parallelogram denoting the strength of the contribution. For the 2.5-eV structure, major contributions come from around the Γ - M - R plane of the BZ, while for the 4-eV structure major contributions come from the central region of the BZ. The contributions to the structures occurring near symmetry directions are also denoted as arrows between initial and final states in the band structure in Fig. 1.

According to the room-temperature optical data for β' -NiAl in Ref. 3, for Al concentrations between 38.4 at. % and 54.8 at. %, the peak of the 2.5-eV structure shifts to lower energies as the Al concentration increases. This downward shift of the 2.5-eV structure can be explained by assuming a rigid-band behavior in which E_F moves upward as the Al concentration increases, resulting in a decrease in the energy of the 2.5-eV transitions which occur between initial states near the Fermi surface and final states above E_F . This rigid-band model assumes

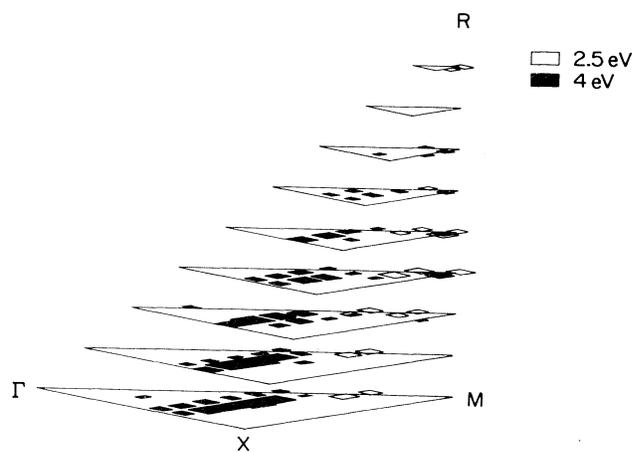


FIG. 5. Regions in the irreducible wedge of the sc Brillouin zone of β' -NiAl contributing to interband transitions in the (2.38–2.52)-eV and (4.15–4.28)-eV spectral regions. Larger parallelograms show the locations of the tetrahedra with the largest contributions (from the product of electric-dipole matrix elements and joint density of states). Smaller parallelograms show weaker transitions.

that due to atomic correlations a d^9 configuration is maintained on each Ni atom independent of the Al concentration.²¹ The structure at about 5.8 eV in the calculated spectrum is mainly due to transitions between initial states with Ni $p-d$ and Al p character well below E_F and final states above E_F with Ni $s-p-d$ and Al $s-p$ character (e.g., bands 3 and 8 in the Γ - M direction). The corresponding structure in the experimental data occurs at about 5.3 eV, which disagrees by about 0.5 eV with the calculational result.

In Fig. 6 the calculated optical conductivity of β' -CoAl is compared with the optical data obtained from KK analysis of the absorptivity measured at 4.2 K in the 0.1–2.5 eV range.⁶ The extrapolation to high energies was achieved by using reflectivity data of Ref. 2 between 2.5 and 6 eV, data used for β' -NiAl to 30 eV, and a power-law extrapolation beyond. The calculated spectrum has several structures below 3 eV caused by interband transitions, located close in energy to each other (0.7, 1.4, 1.6, 2.3, and 2.7 eV). The experimental spectrum also shows several structures at nearly the same energies (0.7, 1.2, 1.7, and 2.3 eV), although there is clearly some quantitative disagreement with the positions and the intensities of the structures. These structures were not resolved in other experimental data taken at room temperatures due to a large Drude background.⁴ At higher energies a broad structure occurs at about 4.3 eV in the experimental spectrum while the calculation produced the corresponding structure at about 5 eV. The calculations by Knab and Koenig¹¹ also show some disagreement with experimental spectra for FeAl, CoAl, and CoGa while showing better agreement for NiAl, as do our results.

The discrepancies between the experimental spectra and the calculational results for both the energy positions and the intensities of the structures, which are slighter in NiAl than in CoAl, might be due to final-state effects for the transitions involving $3d$ states which are known to have strong Coulomb correlations.²² The $d-d$ correlation for the states with large d character is significant for $3d$ systems due to the highly-localized nature of the $3d$ orbit-

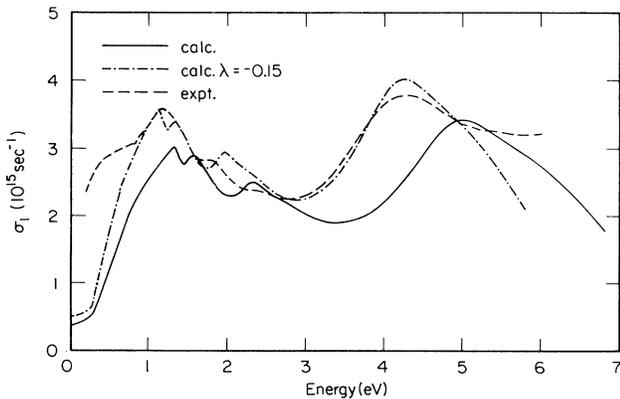


FIG. 6. Comparison of the calculated optical conductivity with the experimental data for β' -CoAl.

als, which maintain strong intra-atomic correlations in the solid. This can lead to significant discrepancies between the experimental results and the theoretical calculations. A very approximate way to treat these effects was adopted following the work of Janak *et al.*²³ They assumed a self-energy correction (shift in the one-electron energy eigenvalues for the excitation) which has the effect of changing the excited-state quasiparticle energies $\hat{E}_n(\mathbf{k})$ relative to the ground-state energies $E_n(\mathbf{k})$ by an amount proportional to $E_n(\mathbf{k}) - E_F$, i.e.,

$$\hat{E}_n(\mathbf{k}) = E_n(\mathbf{k}) + \lambda_{nk}[E_n(\mathbf{k}) - E_F] \quad (3)$$

for the states near E_F . λ_{nk} is determined by the ground-state properties. By assuming λ in Eq. (3) to be a real constant independent of n and \mathbf{k} , the excited-state exchange-correlation potential differs from its ground-state value by a term which is energy dependent but independent of position. Thus, there is no change in the one-electron wave functions so that there is no change in the electric-dipole matrix elements. Furthermore, $\hat{\sigma}_1(\omega)$, the optical conductivity evaluated using the excited-state eigenvalues, is related to σ_1 , the optical conductivity evaluated using the ground-state eigenvalues by

$$\hat{\sigma}_1(\omega) = \frac{1}{1+\lambda} \sigma \left[\frac{\omega}{1+\lambda} \right]. \quad (4)$$

Thus, in addition to supplying a single parameter to fit the experimental spectra, the assumption that λ is constant greatly simplifies the calculation by allowing the use of the ground-state electric-dipole matrix elements. With the parameter λ ($= -0.15$) chosen to make the 5-eV theoretical structure coincide with the 4-eV structure in the experimental data of β' -CoAl the agreement in the low-energy region becomes much better as can be seen in Fig. 6. Janak *et al.*¹³ found that the choice $\lambda = 0.08$ gave a good match between calculated and observed conductivities of Cu. For the transition metals Fe and Ni Laurent *et al.*²⁴ found that negative values of λ ($\lambda = -0.1$ for Fe and $\lambda = -0.12$ for Ni) are needed to produce the best agreement. In the present case, CoAl needs a value of λ larger in magnitude than those used for Fe and Ni to best fit the experimental spectrum.

The interband transitions responsible for the 0.7-eV structure are mainly between states with Co $p-d$ character. The 1.2-eV structure is mainly due to transitions between initial states with Co $p-d$ character and final states with Co d character near E_F (e.g., bands 6 and 7 along the R - X direction and the Γ - M direction). The 2-eV structure is also mainly due to transitions between initial states with Co $p-d$ and Al p character and final states near E_F with Co d character around the M point (bands 4 and 7). The contributions to the structures coming from near-symmetry directions in \mathbf{k} space are also denoted as arrows between initial and final states in the band structure in Fig. 2. The above transitions cannot occur in NiAl because the final-state bands responsible for them are located below E_F in NiAl. The 4-eV structure is mostly due to transitions between states with Co $p-d$ and Al p character well below E_F and states above E_F having Co $s-d$ and Al p character (e.g., bands 2 and 7 in the Γ - X

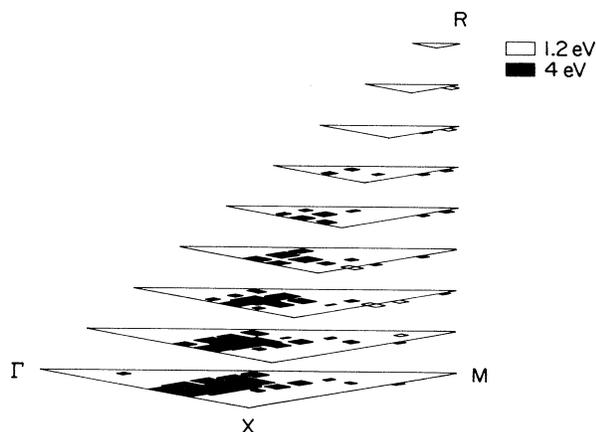


FIG. 7. Regions in the irreducible wedge of the *sc* Brillouin zone of β' -CoAl contributing to interband transitions in the (1.22–1.36)-eV and (4.83–4.96)-eV spectral regions.

direction). The small structure at about 5 eV is mainly due to transitions between initial states with Co *p-d* and Al *p* character well below E_F and final states above E_F with Co *s-p-d* and Al *s-p* character (e.g., bands 3 and 8 in the Γ -*M* direction). The initial and final states of the transitions for the 4- and 5-eV structures are of nearly the same nature as those for the 4- and 5-eV structures in NiAl. Figure 7 shows the regions in the BZ which have major contributions to the 1.2- and the 4-eV structures, respectively. For the 1.2-eV structure the major contribution comes from the *X-M-R* plane, while for the 4-eV structure the major contribution comes from a large volume in the central region of the BZ and the distribution of the strengths is very similar to that of the 4-eV structure of NiAl, indicating that the two structures are caused by almost the same sets of initial and final states in the band structures of both compounds. We believe that the reason for the larger energy shift due to the final-state effect of the 4-eV structure of CoAl (0.7 eV) than the shift of the 4-eV structure of NiAl (0.5 eV) is that the unfilled states of CoAl near E_F have stronger *d* character than those of NiAl, leading to the stronger final-state effect.

III. SUMMARY AND CONCLUSION

The calculated optical conductivity of β' -NiAl agrees well with the experimental spectrum at low-photon energies (< 3 eV). At higher energies there is slight disagreement in peak position and half-width of the structures at about 4 and 5 eV. For β' -CoAl the agreement is poorer than that for β' -NiAl even at low-photon energies. All of the structures found in both compounds involve states with some Ni or Co *d* character for both initial and final states of the transitions. For β' -NiAl the peak at about 2.5 eV is found to be due to transitions between initial states near the Fermi surface and final states well above it while for β' -CoAl there is no corresponding structure involving the same transitions, which are not allowed because of the shift of the Fermi level. Finally for CoAl we investigated a simple approximation for the self-energy corrected excited state energies. We found that a narrowing of the bands [$\lambda = -0.15$ in Eq. (3)] gave better agreement with experiment. The sign and size of this self-energy shift suggests that the excited hole in the valence bands acts locally and pulls the upper conduction-band states to lower energy. Such final-state effects have yet to be thoroughly studied in metallic systems.²⁵

Note added in proof. After this manuscript was submitted, a comprehensive paper on the electronic structure of β' -NiAl appeared [S.-C. Lui, J. W. Davenport, E. W. Plummer, D. M. Zehner, and G. W. Fernando, *Phys. Rev. B* **42**, 1582 (1990)]. Band structures similar to ours were used to interpret extensive photoemission data also reported in the paper. We attempted an empirical correction to our calculation of the optical conductivity by using their derived real part of the self-energy to shift our bands, but there was not significant improvement.

ACKNOWLEDGMENTS

The Ames Laboratory is operated for the U. S. Department of Energy by Iowa State University under Contract No. W-7405-Eng-82. This work was supported by the Director for Energy Research, Office of Basic Energy Science.

¹T. Sambongi, R. Hagiwara, and T. Yamadaya, *J. Phys. Soc. Jpn.* **21**, 923 (1966).

²D. A. Kiewit, J. J. Rechten, and J. O. Brittain, *J. Phys. Soc. Jpn.* **21**, 2380 (1966).

³J. J. Rechten, C. R. Kannewurf, and J. O. Brittain, *J. Appl. Phys.* **38**, 3045 (1967).

⁴D. A. Kiewit and J. O. Brittain, *J. Appl. Phys.* **41**, 710 (1970).

⁵D. J. Peterman, R. Rosei, D. W. Lynch, and V. L. Moruzzi, *Phys. Rev. B* **21**, 5505 (1980).

⁶D. W. Lynch, B. R. Boeke, and D. J. Peterman, *Phys. Rev. B* **25**, 5018 (1982).

⁷J. W. D. Connolly and K. H. Johnson, *Atomic Energy Levels Natl. Bur. Stand. (U.S.) Circ. No. 19* (U.S. GPO, Washington, D.C., 1971), Vol. 323.

⁸V. L. Moruzzi, A. R. Williams, and J. F. Janak, *Phys. Rev. B*

10, 4856 (1974).

⁹C. Müller, H. Wonn, W. Blau, P. Ziesche, and V. P. Krivitskii, *Phys. Status Solidi B* **95**, 215 (1979).

¹⁰R. Eibler and A. Neckel, *J. Phys. F* **10**, 2179 (1980).

¹¹D. Knab and C. Koenig, *J. Phys. C* **2**, 465 (1990). Our work corroborates the results of Knab and Koenig, gives a more complete comparison with experiment, and gives an approximate treatment of self-energy corrections.

¹²W. Blau, J. Weisbach, G. Merz, and K. Kleinstück, *Phys. Status Solidi B* **93**, 713 (1979).

¹³S. P. Kowalczyk, G. Apai, G. Kaindl, F. R. McFeely, L. Ley, and D. A. Shirley, *Solid State Commun.* **25**, 847 (1978).

¹⁴M. Lähdeniemi, E. Ojala, and M. Okochi, *Phys. Status Solidi B* **108**, K61 (1981).

¹⁵P. O. Nilsson, *Phys. Status Solidi* **41**, 317 (1970).

- ¹⁶D. D. Koelling and B. N. Harmon, *J. Phys. C* **10**, 3107 (1977).
- ¹⁷L. Hedin and B. I. Lundqvist, *J. Phys. C* **4**, 2064 (1971).
- ¹⁸O. Jepsen and O. K. Anderson, *Solid State Commun.* **9**, 1763 (1971).
- ¹⁹T. J. Moravec, J. C. Rife, and R. N. Dexter, *Phys. Rev. B* **13**, 3297 (1976).
- ²⁰H. J. Hagemann, W. Gudat, and C. Kunz, *Solid State Commun.* **15**, 655 (1974); *ibid.* **74**, 507 (1976).
- ²¹A similar "rigid-band" behavior can be used to explain the k -dependent shift of phonon anomalies for various Al concentrations. G. -L. Zhao and B. N. Harmon (unpublished).
- ²²T. Bandyopadhyay and D. D. Sarma, *Phys. Rev. B* **39**, 3517 (1989).
- ²³J. F. Janak, A. R. Williams, and V. L. Moruzzi, *Phys. Rev. B* **11**, 1522 (1975).
- ²⁴D. G. Laurent, J. Callaway, and C. S. Wang, *Phys. Rev. B* **20**, 1134 (1979).
- ²⁵N. I. Kulikov, M. Alouani, M. A. Khan, and M. V. Magnitskaya, *Phys. Rev. B* **36**, 929 (1987).